# The Apparent Age of the Time Dilated Universe I: Gyrochronology, Angular Momentum Loss in Close Solar Type Binaries

**Ronald G. Samec, Evan Figg***

## Abstract

In creation time-dilation cosmologies (e.g., those proposed by Humphreys, 1994, and Hartnett, 2007), one major question is: What maximum apparent age should be used to characterize the universe? The 14.7-billion-year answer provided by the Big Bang community should not be accepted due to its false assumptions, which are at odds with biblical history. There are many age-bearing processes (astrochronometers) that we can glean from today's astronomy. Astrochronometers include wind-up times of spiral galaxies, rates of decrease rotation and magnetic activity, and spin-down and coalescence times of binary stars (magnetic braking), star cluster ages (isochron age) and nuclear burning ages (stellar aging on the H-R diagram), rates of visual binary orbital circularization, stellar kinematic ages, white dwarf cooling ages, pulsar spin-down ages (due to gravitational radiation), radio isochron ages from stellar spectra, and others.

In this study, we will explore the subject of gyrochronology: the precise derivation of stellar ages from the rotational period of single solar-type stars and the orbital periods of interacting binaries. As stars and binaries age, magnetic braking steadily steals away angular momentum, and magnetic activity decreases. We seek to include original research from our astronomical observations. In this regard, we present a preliminary analysis of an asynchronous, fast-rotating and near solar-type double contact eclipsing binary (Wilson and Twigg, 1980), AC Piscium from a recent observing run. We also include pertinent interferometric results of fast-spinning single stars. Finally, we attempt a first-ever age estimate of short period solar-type binaries apart from evolutionary time constraints.

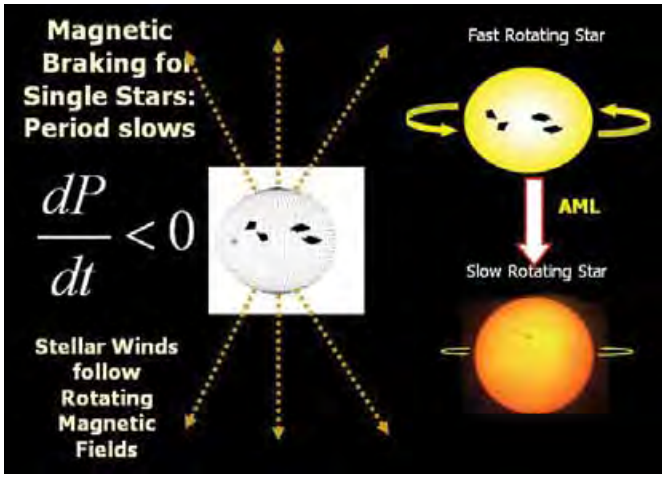


Figure 1. Magnetic braking on single stars. P is the period of rotation. AML is an acronym for Angular Momentum Loss.

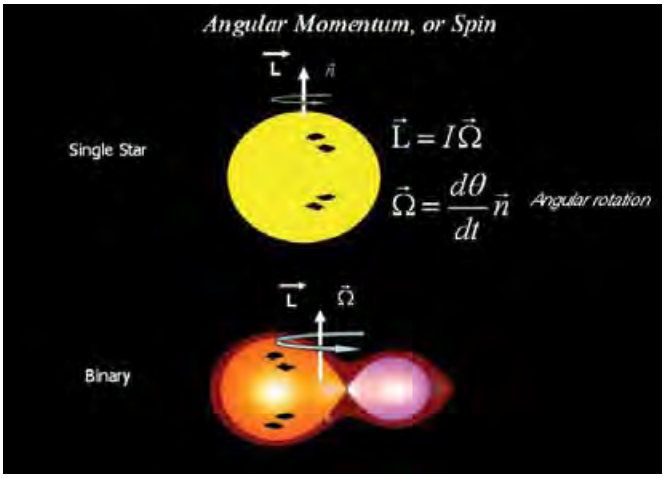


Figure 2. The definitions of angular momentum, L, and angular velocity, Ω.

* Ronald G. Samec, Evan Figg, Bob Jones University, Astronomy Program
Accepted for publication January 14, 2012

## Introduction

We will use the term *astrochronologies* to describe most methods of finding the age of an astronomical object or dating such an event. These schemes are usually corrupted by the assumption that the age of the sun and our solar system is $4.57 \times 10^9$ years, or 4.57 Gigayears (Gyr), as a necessary input. We shall call this the Solar Age Condition (SAC). This is imposed in the age calculation. This is actually the maximum radioisochron age of "primordial" meteors. Due to this lesser-known calibration, derived ages are truly "astronomical." In this particular study, we will point to examples of this in the field of *gyrochronology*, the precise derivation of stellar ages from the orbital period of solar-type stars and interacting binaries.

The RATE project (Vardiman et al, 2005) has demonstrated that the billions of years chronology of isochron dating is faulty, and actual geological ages are nearer to the chronology given to us in the early chapters of Genesis. Here the genealogies sum to give the date of creation about 4000–5000 BC. The discrepancy, thousands of years versus billions of years, is due to an accelerated radioisotope decay rate occurring early in earth's history, whereas standard geology assumes a constant decay rate. This makes the age of the solar system nearer to 7000 years. However, this is the date attributed to earth-bound clocks. In *Starlight and Time* (Humphreys, 1994), general relativity was used for the first time to solve the light-time problem: how can astronomical observations be made of objects billions of light years away in a 7000-year-old universe? Humphreys's answer to this dilemma is that time dilation occurred in the earth-based observational frame. In his first model, earth-based clocks ran slowly when a collapsing white hole event horizon passed the earth. During those moments, light not only came from the deepest realms of space to earth, but physical processes also accelerated throughout the universe. A mature cosmos with a presumed and possibly apparent age of millions or billions of years was left in its wake. This was followed by the complete evaporation of the white hole responsible for the event. Thus, in the frame of reference at cosmological distances, possibly millions to billions of years passed, while in the earth time frame only a few days of time or less were experienced. The question here is this: What is the apparent age experienced by the universe in its time frame? Also, how large a region can be called the "earth time frame," and what happened in nearby regions? So we prefer to pose the question as, "What apparent age can we use to characterize the universe?" The 14.7-billion-year answer provided by the Big Bang community should not be accepted due to its false assumptions, which are at odds with biblical history. We will seek to avoid the SAC in our study wherever possible. Thus, we would like to base our timescales on a natural reference clock (NRC) rather than clocks calibrated with the SAC. Such chronometers include Newtonian orbital periods, the speed of light, and situations where the physical rates, frequencies, velocities, and accelerations are known from observations.

For instance, a recent study was published in *Creation Matters* (Samec, 2011) on the missing intracluster medium (ICM) in globular clusters, which should be created by stellar winds of member stars. We used cluster orbital periods about the Milky Way and the time between orbital passages of the galactic plane as a NRC. We would like to replicate this type of study many times over as we explore age-bearing processes in modern astronomy. One of these, spiral windup times, has been indicated by Humphreys (2001). Others include rotation and magnetic activity and spin-down of solar-type stars and binary star coalescence (magnetic braking), star cluster ages (isochron age) and nuclear burning ages (stellar aging on the H-R diagram), binary star circularization, stellar kinematic ages (stars' dispersal velocity increase with time due to interactions), white dwarf cooling age, pulsar spin-down age (due to gravitational radiation), radio isochron ages from stellar spectra, and others. In each of these studies, we will seek to scale events with a NRC rather than SAC.

## Magnetic Braking

In this study we will explore the area of gyrochronology: the precise derivation of stellar ages from the decay of the orbital period of single solar-type stars and interacting binaries, i.e., magnetic braking. We will explore the magnetic braking of both single stars and close binaries.

### Single Stars

By "solar-type stars," we mean stars that have outer convective zones in the outermost layer. These are called convective *envelopes*. Stars are self-gravitating gaseous spheres that produce energy by continuous nuclear reactions in their cores. The core extends to 0.25 $R_{\odot}$, the radius of the Sun. In the Sun, and other A5 to K type stars, the energy is transported outward by electromagnetic radiation through the radiative zone and then onto a convective zone. For the Sun, the radiative zone extends to 0.71 $R_{\odot}$. Beyond that, the density and opacity is such that energy is transported by swirling convective currents. These swirling plasmas produce the magnetic phenomena visible on the Sun's surface, or photosphere, called the *Active Sun*. This includes coronal loops, granulation, sunspots, faculae, prominences, and flares. The magnetic fields on the Sun are largely bipolar—they consist of two poles, north and south. Fields protrude out of the convective regions beyond the photosphere. These bipolar fields restrain the plasmas and produce dark sunspots that occur in pairs called *bipolar magnetic regions*. The magnetic fields extend outward, especially at the poles, and weaken so that plasmas escape along stiff field lines out to a region called the *Alfven* radius, some 50 solar radii. As the winds, consisting of

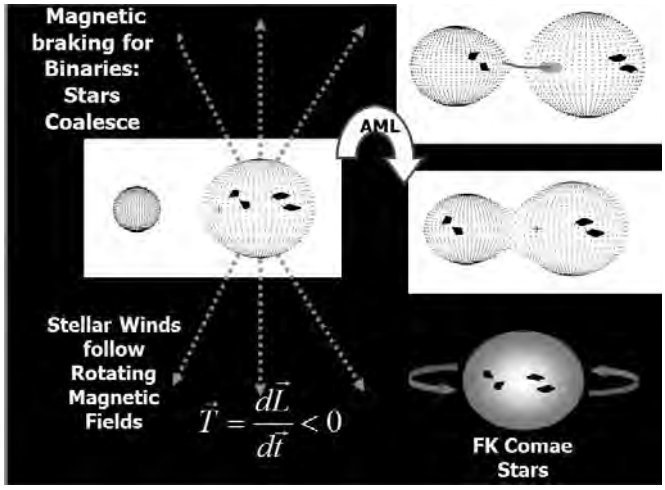


**Figure 3. Close Binaries lose angular momentum. Since they are gravitationally locked, they experience spin-orbit coupling. The entire binary loses angular momentum. As this happens the orbits shrink and, by Kepler's law, the period decreases. The stars become contact binaries and finally coalesce into fast-rotating A-type stars to fast-rotating sub-giants, likes spotted FK Coma stars.**

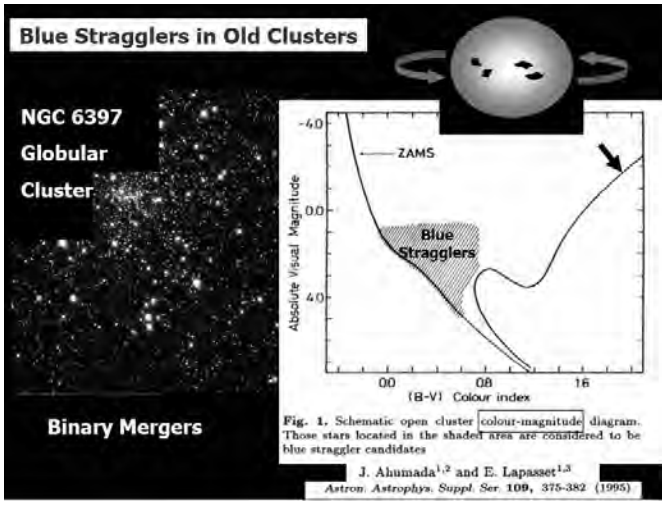


**Figure 4. The isochron of an old cluster is pictured on the H-R or color magnitude diagram. Blue stragglers appear above the turnoff along the abandoned blue part of the zero-age main sequence (ZAMS). The picture of NGC 6397 shows the presence of blue stragglers. A drawing of a fast-rotating FK Coma-type star, blue straggler, is shown in the upper corner.**

mostly protons, escape, they carry away angular momentum, much the same as a spinning speed skater who spreads her arms. The skater's rotation slows down. In the case of stars, the momentum is lost forever as mass is carried away into space.

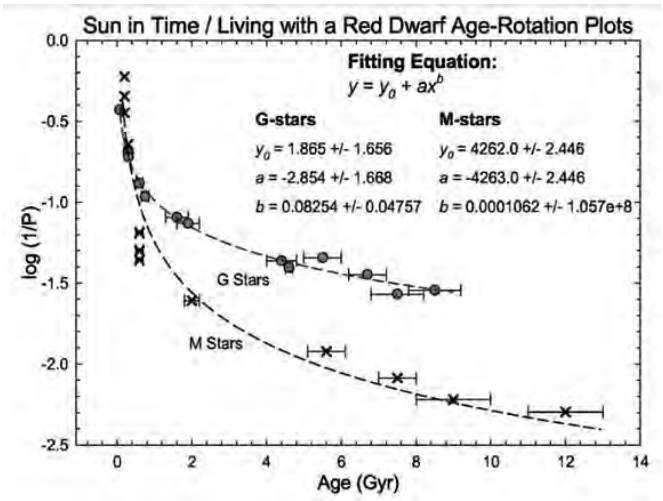


**Figure 5. The period-age relation for single solar analogs and M-type stars determined by linking stars to nearby open clusters with known ages, calibrated with CaII emissions of stars with M67 solar-type stars (Solar age), and from U-V-W space motions (kinematic ages), from isochrones of modern stellar evolution codes (from Guinan and Engle, 2008). P is in days.**

In this way, over time, a fast-rotating, magnetically active star becomes a slow-rotating, less active star like our present-day Sun with its ~25-day rotational period. This process is called magnetic braking (see Figure 1).

Angular momentum, L, for an object orbiting about a single axis is written as

$$\vec{L} = I\vec{\Omega}$$

$$\vec{\Omega} = \frac{d\theta}{dt}\vec{n}$$

*I* is the Moment of Inertia, sometimes called the *rotational inertia*, and Ω is the angular velocity. *I* has to do with the distribution of mass about the axis of rotation, distance r. Vectorally, Ω is the rate of change of angle, θ, in radians per second, times the unit vector directed along the north pole (see Figure 2). *I* can be written as

$$I = \sum_i m_i r^2_i = MK_z^2$$

$K_z$ is known as the radius of gyration, and M is the total mass. The torque, $\vec{\Im}$, is the rate of change of angular momentum.

$$\vec{\Im} = \frac{d\vec{L}}{dt}$$

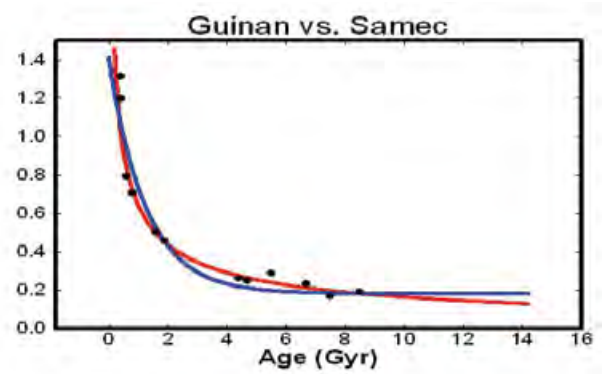


Figure 6. Conversion of Figure 5 to an angular velocity versus age to demonstrate the spin-down due to magnetic braking. The red line is Guinan's power law fit and the blue is the magnetic braking law fit. Both are adequate fits, but the magnetic braking fit follows the theory.

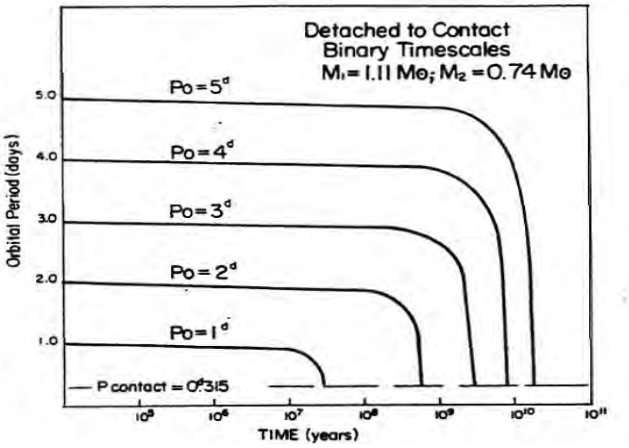


Figure 7. The time needed to brake from a, 1-5 d period binary to a 0.315 period binary with masses of 1.00 to 5.00 (Guinan and Bradstreet, 1988).

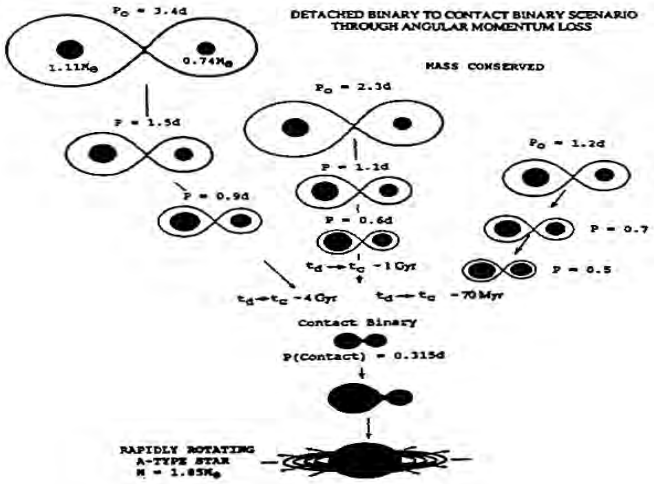


Figure 8. Graphic Depiction of the time evolution of a solar-type binary braking from a, 1-5 d period binary to a 0.315 period binary and on to a coalesced, rapidly rotating single star (Guinan, Bradstreet, and Robinson, 1987).

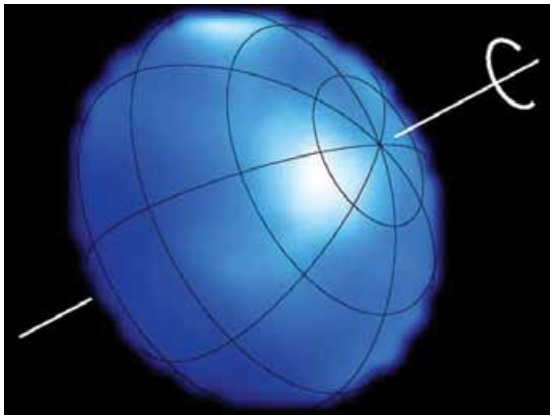

Figure 9. The CHARA-constructed image of Altair. Constructed images of all the tabled stars may be found on the CHARA website: http://www.chara.gsu.edu/CHARA/Slides/CHARAoverview.pdf.

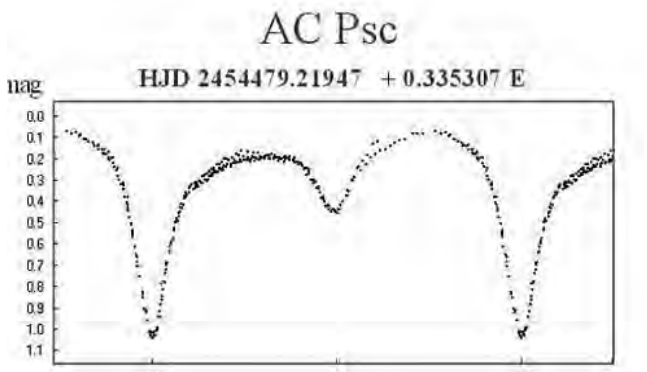


Figure 10. Unfiltered observations by Kryachko et al (2008). Note the hump around phase 0.8 just before the primary eclipse.

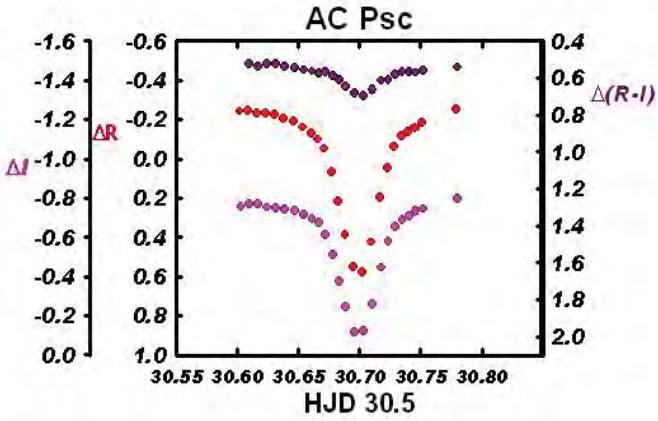


Figure 11. R and I curves, and R-I color index curves taken on HJD 2454730. HJD are "Heliocentric Julian date" observations transformed to the center of the Sun to eliminate light-time effects that would be experienced on the earth due to its orbital motion (when we are closer to the star, the eclipses would take place earlier, etc.).

### Binary Stars

Binary stars consist of two stars that orbit about a common center of mass with a common orbital period. When binaries lose angular momentum, their orbits shrink and the period decreases (see Figure 3). With time, the entire binary steadily loses angular momentum. As this happens, the orbit shrinks and, by Kepler's law, the orbital period shortens. When the atmospheres of the stars touch, the stars are called *contact binaries*. The stars continue to coalesce into fast-rotating single stars such as A-type stars or sub giants, like the spotted FK Coma stars. An example of this phenomenon is found in star clusters where the proximity of stars allows more interacting binaries to form. The magnetic braking process described here is thought to be responsible for the existence of so-called *blue stragglers* in these star clusters. As star clusters age, the turnoff point of the giant branch extending to the right of the main sequence on the H-R diagram shifts to lower and lower masses, leaving a gap above it. Stars are not supposed to appear in this "empty" zone (see Figure 4). Surprisingly, some "young" blue stars do appear here, even in old clusters. These "born-again" stars are called blue stragglers and are thought to be due to binary coalescence. So AML causes *single stars* to slow their rotation and *binaries* to coalesce.

### Astronomical Timescales, Single Stars

Ed Guinan (Guinan & Engle, 2008), in his multi-decade study of the Sun's evolution through time using solar analogs, has provided us with a typical and thorough study that yields gyrochronological ages. These ages are based on the SAC. We have summarized the repercussions of this work in a previous paper (Samec, 2004).

Figure 5 shows the rotational period of solar analogs and M-type stars (which are fully convective from the core to the surface) versus age. Rotational periods decrease with time, presumably due to magnetic braking. The relation is unmistakable. But the ages are all scaled with the astronomical age of our sun. The rate of change of the period dP/dt found from the decay of the period with time will be tied into the decay of the angular momentum later. Here we will tie the angular velocity, $\Omega$, which is proportional to 1/P, to this process through the well-known magnetic braking equation, (1), for single stars (Reed, 2011). The term $r_A$ is the Alfven radius, P is the rotational period, M is the mass at any time, and Mo is the initial mass. The solution to equation (1) is (2). If we assume that the mass loss is constant (R), the solution is equation (3). Since R is negative, the angular velocity decreases with time.

$$\Omega = \frac{2\pi}{P}$$

$$\frac{d\Omega}{dt} = \Omega \frac{dM}{dt} r_A^{\,2} \quad (1)$$

$$\Rightarrow \Omega = \Omega_0 e^{(M-M_0) r_A^{\,2}}, M < M_0 \quad (2)$$

$$or,\ allow$$

$$R = \frac{dM}{dt}$$

$$\Rightarrow \Omega = \Omega_0 e^{R r_A^{\,2} t}, R < 0 \quad (3)$$

We can easily convert Figure 5 to demonstrate this relation (Figure 6). We include our magnetic braking fitting relation and Guinan's power law (which has no scientific basis). Our braking law (with zero point fitting terms) does fit well (equation 4), demonstrating that the theory produces a good fit.

$$\Omega = 1.64 e^{(-0.795t - 0.287)} + 0.181 \quad (4)$$

We note that both of these plots give ages in billions of years, following the SAC, which was used.

### Astronomical Timescales, Binary Stars

Much of the work in the area of binary stars has been done by Bradstreet and Guinan. In their benchmark paper, "Kinematic Clues to the Origin and Evolution of Low Mass Contact Binaries" (Guinan and Bradstreet, 1988), they produce an example plot of the evolution of a binary to a contact configuration with a 0.315 d period. This is given as Figure 7. Again, the models in this section are all calibrated by the SAC ($4.6 \times 10^9$ years). The effect of this is seen in the time axis scales of tens of millions to tens of billions of years. Figure 8 shows a graphic depiction of the same process including the final coalescence into an A-type star.

### Recent Studies in Optical Interferometry

Recent studies of bright (backyard-type) stars have revealed that many are stars rotating at near the centrifugal limit, that is, they are rotating at near break-up velocity! This interesting work has been done at Mount Wilson with the CHARA array (Center for High Angular Resolution Astronomy). For O to about A4V-type stars, this has not been as surprising, since these stars do not have convective atmospheres, and do not have stiff magnetic dipole fields for winds to travel on to cause magnetic braking. So their fast rotations are preserved from their creation. In fact, the author suggests that the attribute of fast rotation could be an attribute of all stars at their creation and is probably the origin

of disks on young stellar objects. (The high rotations cause the formation of disks, which bleed away the excess angular momentum.) Early disks have the appearance of spiral arms. (It could be that this is the origin of galactic spiral arms, that is, the high spin rate of galaxies and their need to lose excess AML and not the presence of dark matter.)

What is surprising is that a number of convective or partially convective stars have been studied in this interferometric work and found to also have this attribute! The observation distinction of convective stars is that their so-called gravity darkening coefficient, $\beta < 0.25$. For radiative stars, $\beta=0.25$. $\beta$ seems to minimize at about 0.08 for deeply convective stars. We summarize the results of this interferometric work in Table I.

These stars are evidently quite young. (Could this be used as evidence for young creation models?) Although it is too early to make any conclusions on stars in general, it appears that the Creator induced fast rotations in many created stars by whatever means, and solar-type stars steadily spin down by magnetic torques induced by out-flowing winds along stiff field lines. If both radiative *and* convective stars retain their high rotations, does this not attest to the youthfulness of these stars?

## AC Piscium, Short Period Asynchronous Rotating Eclipsing Binary

This study of gyrochronology all began when the analysis of a binary revealed two components of a short period binary that have periods of rotation faster than the orbital period. This suggested further work on this phenomena and its affect on the age of the cosmos. Here we give an abbreviated analysis of this binary largely conducted by a senior physics major at Bob Jones University in the 2010–2011 academic year and completed in the summer. Short period systems of this type are nearly always synchronously rotating, so this is evidently an interesting system related to the subject at hand.

### 1. AC Piscium: History and Observations

AC Psc has various identifications, including NSVS14605916, GSC 0584 1274, 2MASS J23213576+0635568, SV* GR 263 (Pinto and Romano, 1973). The position of the variable star (V) is $\alpha(2000) = 23h\ 21m\ 35.776s$, $\delta(2000) = +06^{o}\ 35'\ 57.58"$ (Guide8). It was recently reclassified by ROTSE (http://www.rotse.net/) as an Algol-type binary (IBVS #5699) with the following ephemeris (fitted time of minimum light + orbital period):

$$\mathbf{HJD\ T_{min}\ I} = 2451458.768 + 0.3353\ d \times E \qquad (5)$$

and an R-magnitude range of 13.6 – 14.6 (primary eclipse). Its secondary eclipse had an R-mag of 14.1. It has a difference of depths of eclipse of 0.5 mags. This suggests that it is not a contact binary. It was recently observed by Kryachko et al (2008) with a small scope using no filters. The observations cover 11 nights from October 5, 2001, to July 31, 2003. They determined the improved ephemeris:

$$HJD\ Tmin\ I = 2454479.21947 + 0.335307\ d \times E \qquad (6)$$

(Indeed, amateur creationist astronomers could purchase GO TO scopes and CCD cameras to help us in this work.) Here it is said to be a possible EB (like Beta Lyra), RS CVn system due to the hump following the secondary eclipse. In RS CVn binaries, such spot-induced asymmetries move through the light curve due to differential rotation of various latitudes of the star where the spot happens to occur. Also, it is believed to be the X-ray source 1RXS J232128.6+063633. X-rays arise due to coronal activity in convective stars. Figure 10 shows the light curve they observed.

**Table I. Attributes of Interferometrically Observed Convective Stars.**

| STAR | Spectra | Equatorial Temperature | Rotational Velocity | Ref |
|---|---|---|---|---|
| Altair | A7V | 6860K | 90%–92% of brake up | 1 |
| $\alpha$ Cephei | A9V | 6700K | 93%–94% of brake up | 2 |
| $\alpha$ Ophiuchus | A5V | 7460K | 88.5% of brake up | 3 |
| $\beta$ Cassiopiae | F5V | 6200K | 93% of brake up | 4 |
| Vega | A5V | 7900K | 91% of brake up | 5 |

1 Monnier et al, 2007
2 van Belle et al 2006; Zhao et al 2009
3 Zhao et al 2009
4 Che et al 2011
5 Aufdenberg et al, 2006. Note that T(pole) is 10,15 K0 so Vega is only partially convective.

AC Psc was officially named in the 62nd Name List (1977). Photometric color indices were determined from 2-MASS observations. This gives a J-H = 0.653, H-K = 0.012, or spectral types of K7V and K5V, respectively. We note that these are consistent with each other and are similar to those found from our own photometric measurements.

Four color, B,V,$R_c$,$I_c$ filtered light curves were taken on September, 17–20, 2008, at Lowell Observatory with the 0.81-m reflector with NURO time. Multiband observations enable surface temperature related phenomena to be delineated in simultaneous light curve solutions. For instance, in many cases, we have noted that mass ratios are determined to within 10%, even before radial velocity curves are taken. Our observations were taken with the cryogenically cooled 2KX2K CCD. Some 112 observations of AC Psc were taken in the B-filter, 142 in V, 132 in R and 129 in the R filter.

In Figure 11 is a representative R, I and R-I curve taken on HJD (Heliocentric Julian date) 2454730.

## 2. AC Psc: Period Study

Six times of minimum light (or eclipse timings) calculated from our observations mostly using parabola fits of four primary eclipses, HJD I = 2454730.7000 (±0.0007)d, 24554729.6941 (±0.0006)d, *2454728.6882 (±0.0005)d, 2454727.6821 (±0.0040)d, and 2 secondary eclipses, HJD II= 2454727.8503 (±0.0006)d, 2454728.8564 (±0.0004)d. The starred eclipse was determined by the Wilson code-fitting algorithm. The following improved linear ephemeris as calculated from all data is shown in Figure 12 along with the plotted residuals.

By removing the first point (perhaps an outlier), we were able to determine a reasonable quadratic fit. The residuals and ephemeris are shown in Figure 13. Since the period change is so quick as compared to AML (perhaps 10 X faster), a period increase is taking place, opposite to what would be expected, a dp/dt < 0. The components are apparently separating for a brief time due to the transfer of angular momentum from the primary star to orbital angular momentum of the system. The primary star is evidently not yet coupled (synchronously rotating).

## 3. Finding Charts, Positions, and Standard Magnitudes

The positions of the comparison (C) and check (K) are given in Figure 14 for the sake of future observers. Observations in the differential photometry performed here is in the sense of Δmag = V-C. C-K is used to determine if the comparison star is not varying.

The C-K values were constant throughout the observing interval. C was identified as GSC 0584 0247. Its position is α(2000) = 23h 21m 35.576s and δ(2000) = +06° 39' 10.54". K is GSC 0584 0776. Its position is α(2000) = 23h 21m 50.484s, and δ(2000) = +06° 40' 04.12", B-V = 0.332.

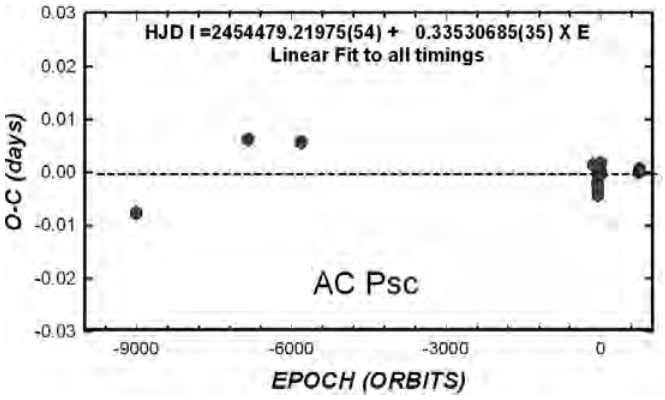


**Figure 12. Improved linear ephemeris was calculated from all available data of AC Psc.**

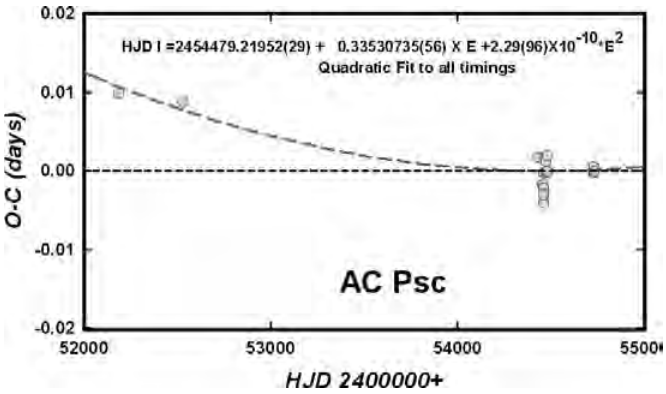


**Figure 13. Quadratic ephemeris showing possible increasing period.**

Landolt standard stars were observed on all four nights with good results, and the magnitudes of the V, C, and K stars were transformed to the standard Johnson-Cousins system using normal techniques. These confirmed that the primary had a temperature of about 4000K as was used in our light-curve solution (photometric spectral type K7.5). The C and K stars were both early G type stars. Average values are shown in Table II.

## 4. Phased Light Curves

We phased the light curves with the linear ephemeris given in Figure 15; mag versus phase is given. The BVRI light curves are EA/EB type (EA-Algol type) with their large difference in eclipse amplitudes when comparing the primary to the secondary eclipse. This may indicate a semidetached configuration (one star filling its critical surface and the other under filling). The light curves also show unsymmetrical effects (about the

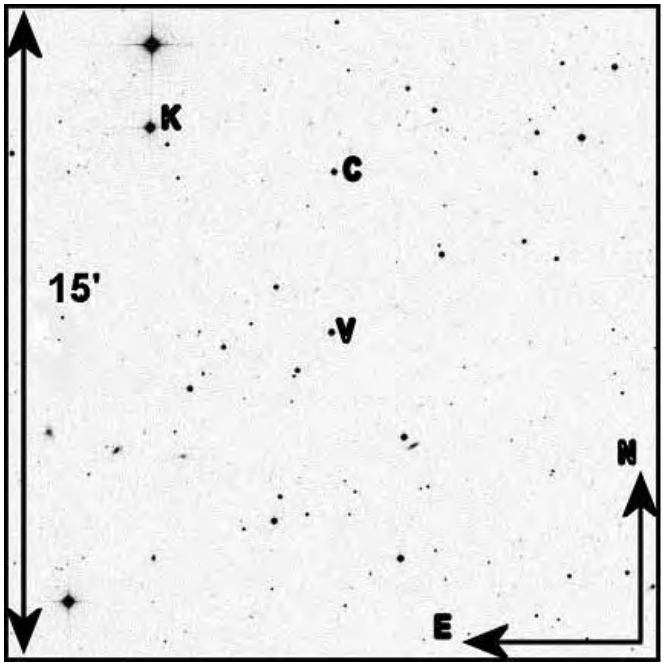


**Figure 14. Finding Chart for the variable (V), comparison (C) and the Check star (K).**

center of eclipses) due to spots and unknown phenomena. We note that the "hump" observed in the Figure 10 curve is now depressed, possibly due to variable stream spot.

## 5. Synthetic Light Curve Solution

The phased light curves, B, V, R, and I, were firsthand modeled with Binary Maker 3.0 (Bradstreet and Steelman, 2002). We sought to produce nearly consistent fits. The parameters from these fits were averaged and entered along with the light curves into the 2004 Wilson Code (Wilson and Devinney, 1971; Wilson, 1990, 1994; Van Hamme and Wilson, 2003). We followed this by attempting a simultaneous 4-color synthetic light curve solution. We tried mode 4 and 5 (semidetached with a either component as $M_1$, the component at superior conjunction at primary eclipse), third light, and spots with poor results. Next, we tried to vary the "F" parameter (nonsynchronous rotation, and double contact mode 6). This immediately led to solutions, albeit poor ones. Due to the confusion as to the actual mode of the binary, we ran our solutions in mode zero, which allows unconstrained models. With this, we allowed the F parameters to continue to iterate. We also began solutions at various fixed mass ratios or q values to determine the lowest residual solution. This q-search resulted in the diagram in Figure 16.

The mass ratio minimized at near q=0.45. Next, we allowed the q-value to adjust, and the Wilson code converged on our final solution. Our best BVRI solution is found to be a near double contact with a primary just under filling its rotating lobe, 97%, and spinning at 1.36 times the orbital Ω. It is probably releasing a gas stream, producing a weak hot spot on the secondary. This is also confirmed since the location of the hot spot (caused by a gas stream) obeys the Coriolis force, and it is placed at near 90° latitude. In addition, the secondary is spun

**Table II. Standard Magnitudes C, V (at quadratures), K.**

| | V | B-V | V-R | R-I | V-I | Sp. type |
|---|---|---|---|---|---|---|
| K | 11.34 | 0.62 | 0.32 | 0.33 | 0.68 | G1.0(1.5) |
| ± | 0.06 | 0.03 | 0.01 | 0.03 | 0.03 | |
| V phase | | | | | | |
| 0.00 | 14.83 | 1.31 | 0.82 | 0.93 | 1.75 | K7.5(2.0) |
| ± | 0.20 | 0.02 | 0.02 | 0.02 | 0.03 | |
| 0.25 | 14.30 | 1.45 | 0.70 | 0.80 | 1.74 | K6.5(0.3) |
| ± | 0.10 | 0.02 | 0.03 | 0.22 | 0.11 | |
| 0.50 | 14.30 | 1.16 | 0.69 | 0.79 | 1.57 | K7.5(1.0) |
| ± | 0.07 | 0.02 | 0.02 | 0.02 | 0.03 | |
| 0.75 | 14.25 | 1.23 | 0.71 | 0.83 | 1.64 | K7(1) |
| ± | 0.01 | 0.04 | 0.02 | 0.01 | 0.04 | |
| C | 14.08 | 0.57 | 0.49 | 0.35 | 0.69 | G2.0(1.5) |
| ± | 0.05 | 0.02 | 0.02 | 0.01 | 0.01 | |

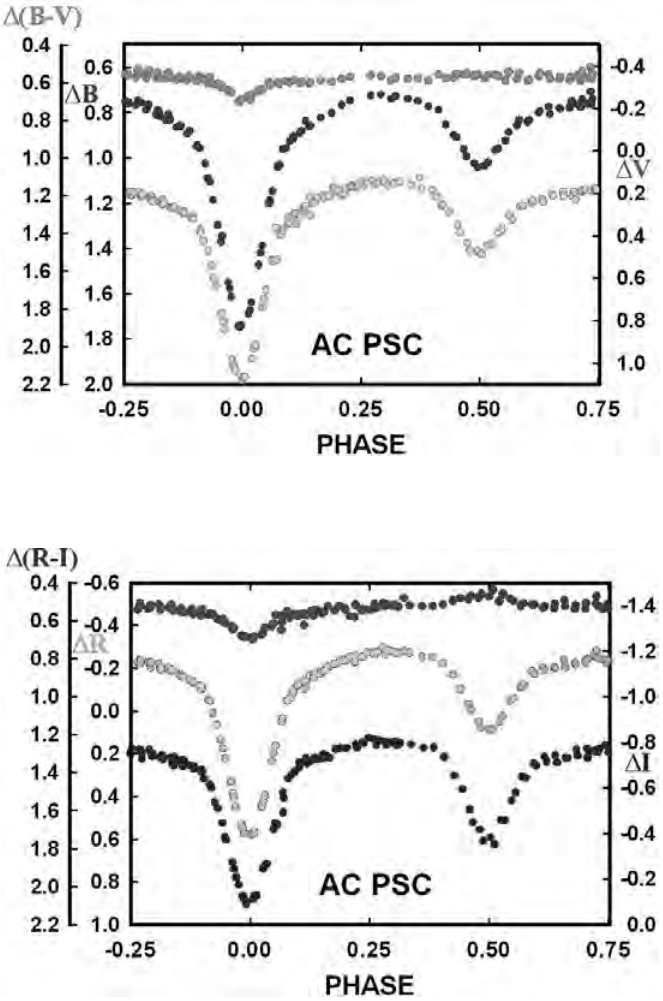


**Figure 15a, b. AC Psc, B,V,R,I Delta Mag light curves phased with equation in Figure 13.**

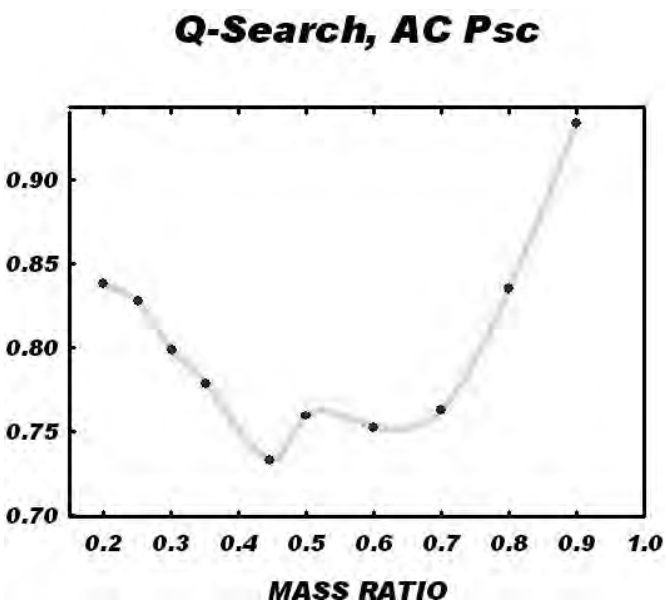


**Figure 16. Mass ratio (Q) search of models to determine the best fit mass. The mass ratio minimizes at about 0.45.**

up, at 1.42 times the orbital Ω. Some solution parameters are given in Table III.

In Figure 17, we show the light-curve solutions overlaying the data. The surface models are given in Figure 18.

AC Psc is a detached system composed of nonsynchronously spinning components. The secondary component is presently spun up by a stream from the primary at 1.42 X the synchronous rate. Notably, the primary is still slightly spun up at 1.36 X the synchronous rate, which means that it was spinning at a faster rate at its creation like many other single stars. This is unusual. The usual near-contact binary is synchronously rotating due to gravitational drag. However, the asynchronous rotations should slowly die out over time and the system will come into contact as a normal "over contact" binary. The driving mechanism for this assumed process is the torque supplied by out-flowing winds along "stiff" magnetic field lines originating from the solar-type stars.

## Age Determination

We now embark on the climax of the paper, the determination of the age of close eclipsing binaries undergoing AML. During the past 25 years, we have been observing binaries undergoing AML with negatively measured dP/dt's, especially from those of solar type. From these we can obtain an average AML loss. A listed tabulation is given in Table IV. These results are *independent* of the usual SAC calibration. Here our results are dependent only on NRC's, orbital periods. In Figure 19, we show a typical O-C residual plot from eclipse timings. This type of calculation gives the rate of period decrease of T= $-Q*E^2$ +PxE +To, the standard form of quadratic ephemeredes, i.e., the new eclipse happens at time T after so many epochs, or orbits, E, added to the initial eclipse, with a quadratic, $E^2$, "deceleration term." This acts the same way as a Newtonian kinematical calculation with a deceleration, y = -1/2 $at^2$ + bt +c, like the motion of a car with its brakes on. In this case the period or the angular momentum is decelerating.

In this calculation we will use AML equations from the analysis of Guinan and Bradstreet (1988). But we use only those free of the SAC. Equation (6) gives the orbital angular momentum of a gravitationally coupled binary star.

$$L_{orb} = 1.242 \times 10^{52} q(1+q)^2 (M)^{5/3} P_{orb}^{\frac{1}{3}} \quad cm^2 gm/s \quad (6)$$

**Table III. Some Parameters of the BVRI simultaneous solution of AC Psc.**

| | |
|---|---|
| Inclination = 79.7 ± 0.1 $^{o}$ | Star 1: Less Massive Component<br>Star 2: More Massive Component |
| $T_1$ = 2899± 18 K, $T_2$ = 4040 K | Omega Potentials 1: 3.073±0.005<br>Omega Potentials 2: 3.144±0.059 |
| gravity coefficient 1,2 = 0.32, 0.32, reflection 1,2 = 0.50 | Mass Ratio: $M_1/M_2$ = 0. 4458 ± 0.0016 |
| Near Double Contact, nonsynchronous rotation,<br>$F_1$ =1. 362±0.019 (x orbital rate)<br>$F_2$ = 1. 415±0.011 | Fill-out: Fill-out Star 1= 0.967,<br>Fill-out Star 2= 0.945<br>HJD0=2454728. 68770±0.00011<br>Period=0. 335331d±0.000029 |
| Spot Parameters:<br>Colatitude: 81±1$^{o}$, Longitude:48±5$^{o}$ | Radius: 10.2±0.3 $^{o}$,T-Factor: 1.16±0.01 |
| Normalized Flux Ratios: $L_1/(L_1+L_2)$-I,R,V,B:<br>0.610±0.004, 0.524±0.005, | 0.510±0.003, 0.461±0.004 |

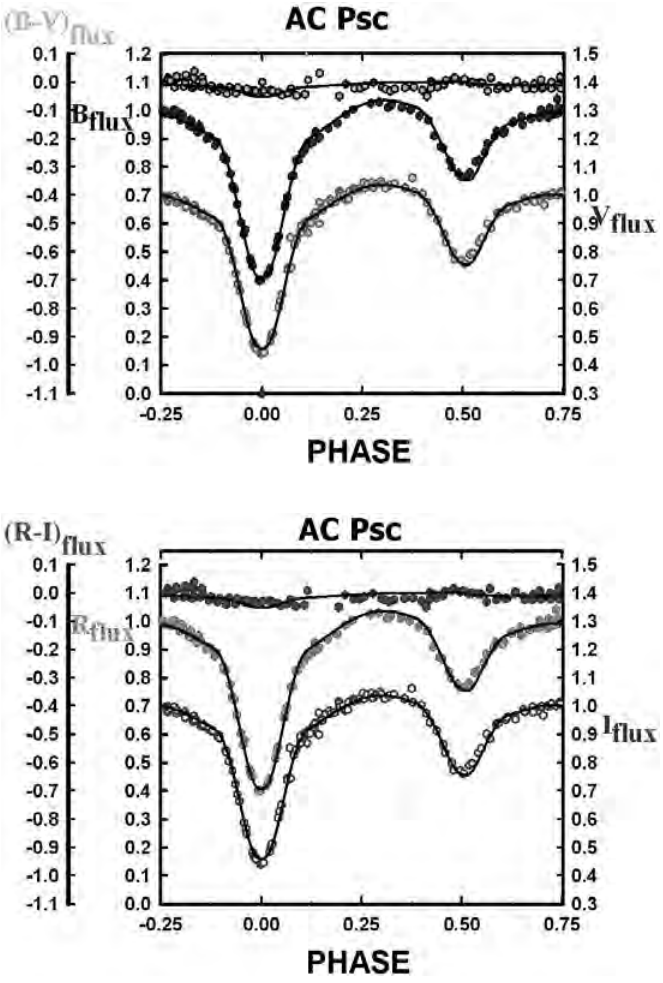


**Figure 17a, b. AC Psc, B,V normalized fluxes overlaid (upper). R,I normalized fluxes also overlaid. B,V,R,I are simultaneous solutions. The first figure has a drawing of the gas stream included for illustration.**

Taking the derivative, assuming no mass transfer and an insignificant mass loss, the torque, $\Im$, becomes:

$$\Im = \frac{dL}{dt} = 4.1\times10^{51} q(1+q)^{-2} M^{\frac{5}{3}} P_{orb}^{-2/3} \frac{dP_{orb}}{dt} cm^2 gm/s^2 \quad (7)$$

where, M is in solar masses, P in days, dP/dt in days/year. Ages, Δt, are calculated from this simple relation:

$$\Delta t = \frac{\Delta L}{\Im}$$

In Tables IV, V, and VI we give the numerical results of our studies.

## Conclusion

We find that the actual determination of the rate of angular momentum loss has a much greater effect on the ages of short period binaries than supposed by the binary star community. Given average values of AML and assuming that we can neglect the small changes in mass over the lifetime of the short-period binaries (Maceroni and Rucinski, 2000), and that these binaries begin their lifetime with periods of 10 days or less (Maceroni and Rucinski, 2000; Guinan and Bradstreet, 1988; Kroupa and Burkert, 2001), their apparent ages *average* from about 300,000 to 700,000 years, whose range actually includes ages as low as hundreds of years. (We could use starting periods much larger than this and still arrive at ages much smaller than that of Bradstreet and others.) The ages are seen to be far less than

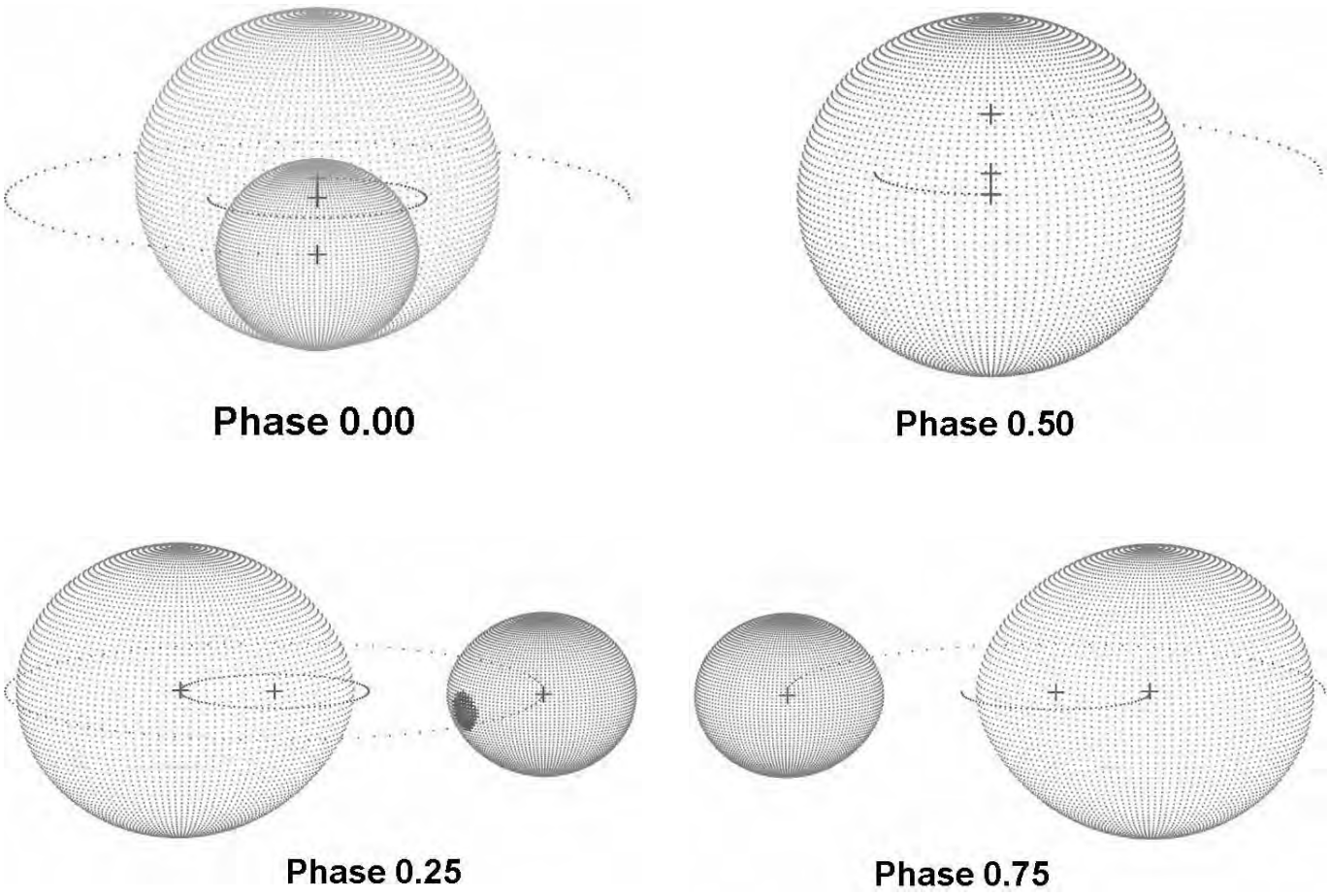


**Figure 18. Surface models of the best BVR solution at quadratures. On the 0.25 phase model, a stream has been added for illustration.**

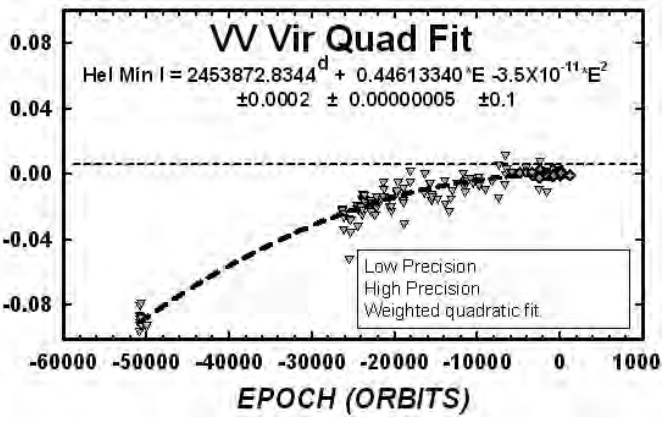


**Figure 19. Our observation and calculation from previous eclipse timings shows that the orbit of VV Vir is decaying. Since this system is of solar type, we conclude that the period decrease and the angular momentum loss is negative. We included this binary in our calculation of the age of such binaries.**

the multibillion-year scenarios painted by binary star researchers (less than a thousandth!). In fact, the range easily includes the biblical age of the solar system, 7000 years, depending on the initial created orbital periods. We observe that all of these objects are local (all within ~1000 parsecs or ~3000 ly) and *not cosmological, deep-space objects*. This may validate the notion that all nearby objects partook in the same dilation effects as the earth during Creation Week and that they all have ages measured in earth time on the order of 10,000 years, nearly the same as we find for solar system objects such as that of Jupiter and interplanetary dust. In the *Publications of the Astronomical Society of Japan* (2009), Tian et al. noted that the rate of decay is "1–2 orders of magnitude faster" than equations by Guinan and Bradstreet predict. Although this should be 3–4 orders, it confirms the thesis of this paper.

We believe that this paper gives physical confirmation of the youthful age of at least the nearby universe. *"For in six days*

**Table IVa. Results of 25 Years of Observing Solar Type Binaries AML**

| | dp/dE (d/E) | dP/dt (d/yr) | period (d) | Est.Spec. Type | $M_1$ (MẎ) | $M_2$ | M |
|---|---|---|---|---|---|---|---|
| AK CMi | -5.000000E-11 | -7.746700E-14 | 0.56589640 | A3 | 2.40 | 1.56 | 3.96 |
| AT Aqr | -3.900000E-11 | -4.036458E-14 | 0.37802984 | G5 | 0.92 | 0.33 | 1.25 |
| BE Cep | -1.600000E-11 | -1.859084E-14 | 0.42439404 | K1 | 0.77 | 0.52 | 1.29 |
| BM UMa | -5.400000E-08 | -4.009828E-11 | 0.27122032 | K3 | 0.73 | 0.37 | 1.10 |
| BX Peg | -1.060000E-10 | -8.138137E-14 | 0.28042024 | G8 | 0.84 | 0.31 | 1.15 |
| CN And | -9.800000E-11 | -1.241709E-13 | 0.46279007 | F6 | 1.30 | 0.50 | 1.80 |
| EH Hydra | -1.600000E-11 | -1.211822E-14 | 0.27663622 | G6 | 0.91 | 0.29 | 1.20 |
| EK Com | -2.050000E-11 | -1.496802E-14 | 0.26668637 | K1 | 0.77 | 0.24 | 1.01 |
| GSC 2537 -0520 | -1.610000E-10 | -1.635512E-13 | 0.37103770 | G5 | 0.92 | 0.15 | 1.07 |
| HM Mon | -1.800000E-11 | -2.008706E-14 | 0.40760000 | G2 | 1.00 | 0.59 | 1.59 |
| V1128 Tau | -3.400000E-11 | -2.842621E-14 | 0.30537273 | G3 | 1.00 | 0.51 | 1.51 |
| V361 Lyr | -3.600000E-11 | -3.051634E-14 | 0.30961373 | F8 | 1.26 | 0.87 | 2.13 |
| V524 Mon | -1.100000E-11 | -8.541482E-15 | 0.28361604 | G8 | 0.88 | 0.42 | 1.30 |
| V803 Aql | -9.000000E-11 | -6.490916E-14 | 0.26342299 | K3 | 0.73 | 0.73 | 1.46 |
| V965 Cyg | -6.500000E-11 | -1.139955E-13 | 0.64056706 | A3 | 2.45 | 1.59 | 4.04 |
| VV CVn | -3.139000E-09 | -4.579993E-12 | 0.53292205 | F2 | 2.60 | 1.30 | 3.90 |
| VV Vir | -3.500000E-11 | -4.275063E-14 | 0.44613340 | G0 | 1.05 | 0.45 | 1.50 |
| XZ CMi | -3.500000E-11 | -5.546414E-14 | 0.57880796 | F3 | 1.50 | 1.25 | 2.75 |
| Average | -3.220528E-09 | -2.531976E-12 | 0.39250929 | | 1.22 | 0.67 | 1.89 |

*the LORD made heaven and earth, the sea, and all that in them is, and rested the seventh day: wherefore the LORD blessed the sabbath day, and hallowed it*" (Exodus 20:11).

## Acknowledgments

We wish to thank Lowell Observatory for their allocation of observing time and the Creation Research Society for their generous support of this project.

## References

Aufdenberg, J.P., A. Mérand, V. Coudé du Foresto, O. Absil, E. Di Folco, P. Kervella, S.T. Ridgway, D.H. Berger, T.A. ten Brummelaar, H.A., McAlister, J. Sturmann, L. Sturmann, and N.H. Turner. 2006. First results from the Chara Array. Vii. Long-baseline interferometric measurements of Vega consistent with a pole-on, rapidly rotating star. *Astrophysical Journal* 645: 664–675.

Bradstreet, D.H., and E.F. Guinan. 1994. Stellar mergers and acquisitions: the formation and evolution of W Ursae Majoris Binaries. In Shafter, A.W. (editor), *Interacting Binary Stars: A Symposium Held in Conjunction with the 105th Meeting of the Astronomical Society of the Pacific, San Diego State University, 13–15 July 1993*, pp. 228–243. Astronomical Society of the Pacific Conference 56.

Bradstreet, D.H., and D.P. Steelman. 2002. Binary Maker 3.0—an interactive graphics-based light curve synthesis program written in Java. *Bulletin of the American Astronomical Society* 34:1224.

Che, X., J.D. Monnier, M. Zhao, E. Pedretti, N. Thureau, A. Mérand, T. ten Brummelaar, H. McAlister, S.T. Ridgway, N. Turner, J. Sturmann, and L. Sturmann. 2011. Colder and hotter: interferometric imaging of β Cassiopeiae and αLeonis. *Astrophysical Journal* 732: 68 (13 pp).

Guinan, E.F., D.H. Bradstreet, and C.R. Robinson. 1987. The W Ursae Majoris systems: the senior citizens of close binaries. *Bul-*

**Table IVb. Results, Continued**

| | $L_2$ (today) | $q=M_2/M_1$ | dL/dt | $L_1$, 5 d (initial) | $L_1$, 8d (initial) | $L_1$, 10d (initial) |
|---|---|---|---|---|---|---|
| | 1.825E+51 | 0.65 | -8.017E+40 | 1.613E+52 | 2.580E+52 | 3.226E+52 |
| | 1.450E+50 | 0.36 | -1.228E+38 | 1.918E+51 | 3.068E+51 | 3.835E+51 |
| | 2.146E+50 | 0.68 | -9.506E+37 | 2.528E+51 | 4.046E+51 | 5.057E+51 |
| | 9.582E+49 | 0.50 | -1.666E+41 | 1.766E+51 | 2.826E+51 | 3.533E+51 |
| | 9.548E+49 | 0.37 | -3.093E+38 | 1.702E+51 | 2.724E+51 | 3.405E+51 |
| | 3.406E+50 | 0.39 | -1.713E+39 | 3.680E+51 | 5.888E+51 | 7.360E+51 |
| | 9.262E+49 | 0.31 | -4.932E+37 | 1.674E+51 | 2.678E+51 | 3.348E+51 |
| | 6.600E+49 | 0.31 | -2.693E+37 | 1.237E+51 | 1.980E+51 | 2.475E+51 |
| | 7.050E+49 | 0.17 | -1.210E+38 | 9.500E+50 | 1.520E+51 | 1.900E+51 |
| | 2.816E+50 | 0.59 | -2.760E+38 | 3.454E+51 | 5.527E+51 | 6.908E+51 |
| | 1.868E+50 | 0.51 | -4.824E+38 | 3.059E+51 | 4.894E+51 | 6.118E+51 |
| | 3.605E+50 | 0.69 | -3.596E+39 | 5.822E+51 | 9.315E+51 | 1.164E+52 |
| | 1.302E+50 | 0.47 | -7.180E+37 | 2.296E+51 | 3.673E+51 | 4.591E+51 |
| | 1.691E+50 | 1.00 | -2.189E+39 | 3.210E+51 | 5.136E+51 | 6.420E+51 |
| | 2.144E+51 | 0.65 | -7.332E+40 | 1.674E+52 | 2.678E+52 | 3.347E+52 |
| | 1.564E+51 | 0.50 | -2.825E+42 | 1.467E+52 | 2.348E+52 | 2.935E+52 |
| | 2.521E+50 | 0.43 | -2.771E+38 | 2.825E+51 | 4.521E+51 | 5.651E+51 |
| | 1.055E+51 | 0.83 | -7.782E+39 | 9.114E+51 | 1.458E+52 | 1.823E+52 |
| Average | 5.050E+50 | 0.52 | -1.757E+41 | 5.154E+51 | 5.154E+51 | 1.031E+52 |

*letin of the American Astronomical Society* 44:1085.

Guinan, Edward F., and David H. Bradstreet. 1988. Kinematic clues to the origin and evolution of low mass contact binaries, formation and evolution of low mass stars. In Dupree, A.K., and M.T.V.T. Lago (editors), *Proceedings of a NATO Advanced Study Institute, Held at Viana do Castelo, Portugal, September 21 - October 2, 1987*, NATO Advanced Science Institutes (ASI) Series C, Volume 241 pp. 345–375. Kluwer, Dordrecht, The Netherlands.

Guinan, E.F., and S.G. Engle. 2008. The sun in time: age, rotation, and magnetic activity of the sun and solar-type stars and effects on hosted planets. In Mamajek, E.E., and D. Soderblom (editors), *The Ages of Stars.* Proceedings IAU Symposium No. 258, 2009, International Astronomical Union.

Hartnett, J.G., 2007. *Starlight, Time and the New Physics*. Creation Ministries International, Adelaide, Australia.

Humphreys, D.R.1994. *Starlight and Time*. Master Books, Green Forest, AR.

Humphreys, D.R., 2001. Evidence for a young world. Impact #384. Institute for Creation Research, Dallas, TX.

Kryachko, T., A. Samokhvalov, B. Satovskiy, D. Denisenko, and A.V. Khruslov. 2008. Variability of AC Psc. *Peremennye Zvezdy Prilozhenie*, vol. 8, no. 17.

Kroupa, Pavel, and Andreas Burkert. 2001. On the origin of the distribution of binary star periods. *Astrophysical Journal* 555:945–949.

Maceroni, C., and S.M. Rucinski. 2000. Magnetic braking in solar-type close binaries. In Jankovics, I., J. Kovács, and I. J. Vincze (editors), *Workshop on the Sun and Sun-like Stars, 9–11 August 1999*, pp. 15–24. Gothard Astrophysical Observatory, Szombathely, Hungary.

Monnier, J.D., M. Zhao, E. Pedretti, N. Thureau, M. Ireland, P. Muirhead, J.-P. Berger, R. Millan-Gabet, G. Van Belle, T. ten Brummelaar, H. McAlister, S. Ridgway, N. Turner, J. Sturmann, L. Sturmann, and D. Berger. 2007. Imaging the surface of Altair. *Science* 317:342–345.

**Table V. Time (years) to change from 10-, 8-, and 5-day periods to present orbital periods.**

| | Age (years) 5d | Age (years) 8d | Age (years) 10d |
|---|---|---|---|
| | 5.65E+03 | 9.48E+03 | 1.20E+04 |
| | 4.58E+05 | 7.55E+05 | 9.52E+05 |
| | 7.71E+05 | 1.28E+06 | 1.61E+06 |
| | 3.18E+02 | 5.19E+02 | 6.54E+02 |
| | 1.65E+05 | 2.69E+05 | 3.39E+05 |
| | 6.18E+04 | 1.03E+05 | 1.30E+05 |
| | 1.02E+06 | 1.66E+06 | 2.09E+06 |
| | 1.38E+06 | 2.25E+06 | 2.83E+06 |
| | 2.30E+05 | 3.80E+05 | 4.79E+05 |
| | 3.64E+05 | 6.02E+05 | 7.61E+05 |
| | 1.89E+05 | 3.09E+05 | 3.90E+05 |
| | 4.81E+04 | 7.89E+04 | 9.94E+04 |
| | 9.56E+05 | 1.56E+06 | 1.97E+06 |
| | 4.40E+04 | 7.19E+04 | 9.05E+04 |
| | 6.31E+03 | 1.06E+04 | 1.35E+04 |
| | 1.47E+02 | 2.46E+02 | 3.12E+02 |
| | 2.94E+05 | 4.88E+05 | 6.17E+05 |
| | 3.28E+04 | 5.51E+04 | 6.99E+04 |
| Average | 3.34E+05 | 5.49E+05 | 6.92E+05 |

**Table VI. Average, Maximum and Minimum Results**

| | Age (years) | | |
|---|---|---|---|
| | 5d Initial Period | 8d Initial Period | 10d Initial Period |
| Average | 330,000 | 550,000 | 690,000 |
| Maximum | 1,380,000 | 2,250,000 | 2,830,000 |
| Minimum | 100 | 200 | 300 |


Observation of Variables. 2006. *Information Bulletin on Variable Stars* #5699.

Pinto, G., and G. Romano. 1973. Researches with the Schmidt telescopes VII - variable stars in the field in RA = 23h 17m, D = + 7° 40' (Pegasus). *MmSAI* 44:273.

Reed, P.A. 2011. Observing mass transfer in a neglected interacting binary star. AAS Meeting #218, #122.04. *Bulletin of the American Astronomical Society* 43:2011.

Samec, R.G. 2004. The sun in time. *Journal of Creation* 18:8–9.

Samec, R.G. 2011. Where is the ICM in globular clusters? *Creation Matters* (in press).

Samec, R.G., C.M. Labadorf, G.A. Behn, H.A. Chamberlain, D.R. Faulkner, and W. Van Hamme. 2008. Photometric analysis and 60 year period study of the detached but near contact system, VV Virginis. *Astronomical Journal* 136:1667–1676.

*62nd Name-List of Variable Stars.* 1977. *Information Bulletin on Variable Stars* #1248.

Tian, Yongpo; Xiang, Fuyuan; Xie, Wenli; Tao, Xia, Period Change and Possible Magnetic Braking in WY Cancri, *Publications of the Astronomical Society of Japan.* 2009, Vol.61, No.4, pp. 675–677.

van Belle, G.T., and D.R. Ciardi, T. ten Brummelaar, H.A. McAlister, S.T. Ridgway, D.H. Berger, P.J. Goldfinger, J. Sturmann, L. Sturmann, N. Turner, A.F. Boden, and R.R. Thompson. 2006. First results from the Chara Array. Iii. Oblateness, rotational velocity, and gravity darkening of Alderamin. *Geophysics Journal* 637:494–505.

van Hamme, W.V., and R.E. Wilson. 2003. Stellar atmospheres in eclipsing binaries. *GAIA Spectroscopy, Science and Technology*, ASP Conference Series, Vol. 298:323–328.

Vardiman, L., A. Snelling, and E.F. Chaffin. 2005. *Radioisotopes and the Age of the Earth, Vol. 2*. Institute for Creation Research and Creation Research Society, San Diego, CA and Chino Valley, AZ.

Wilson, R.E., and E.J. Devinney. 1971. Realization of accurate close-binary light curves: application to MR Cygni. *Astrophysical Journal* 166:605–619.

Wilson, R.E., and L.W. Twigg. 1980. On the existence of double contact binaries. In Plavec, M.J., D.M. Popper, and R.K. Ulrich, (editors), *Close Binary Stars–IAU Symposium 88*, pp. 263–268. International Astronomical Union, Toronto, ON.

Wilson, R. E. 1990. Accuracy and efficiency in the binary star reflection effect. *Astrophysical Journal* 356:613–622.

Wilson, R. E. 1994. Binary-star light curve models. *Publications of the Astronomical Society of the Pacific* 106:921–941.

Zhao, M., J.D. Monnier, E. Pedretti, N. Thureau, A. M´erand, T. ten Brummelaar, H. McAlister, S.T. Ridgway, N. Turner, J. Sturmann, L. Sturmann, P.J. Goldfinger, and C. Farrington. 2009. Imaging and modeling rapidly rotating stars: α Cephei and α Ophiuchi. *Astrophysical Journal* 701:209–224